

Profile Stabilization in Slow and Millisecond Pulsars

Mateus M. Teixeira¹, Isabel Kloumann² & Joanna M. Rankin¹

¹*Department of Physics, University of Vermont, Burlington, VT 05405**

²*Cornell University, Ithaca, NY*

Accepted 2012 month day. Received 2012 month day; in original form 2012 July 24

ABSTRACT

Correlation methods are used to examine the profile stabilization of both normal and millisecond pulsars. A number of the pulsars stabilized in a characteristic manner that shows a “parabolic” dependence—rationalizing earlier findings that showed power-laws of two different slopes. For the remaining objects, the distorting effects of mode changes or other profile dynamics are apparent in the correlations.

Key words: miscellaneous – profile stabilization – pulsar timing – methods: correlations, data analysis – pulsars: general, survey, millisecond

1 INTRODUCTION

This paper reports efforts over the last two years to measure and characterize the average profile stabilization rate for a group of pulsars that includes both well studied slow objects as well as some faster and even a few millisecond pulsars. For this analysis, we adopt the methods developed by Helfand *et al.* (1975; hereafter HMTIII) and later employed by Rathnasree & Rankin (1995; hereafter RR95) for groups of slow pulsars. The procedure involves the computation of cross-correlation functions (hereafter CCF) between a pulsars global average profile and subaverage profiles computed from varying numbers of its pulses. The values of the average correlation coefficient as a function of subaverage profile length then provide a “snapshot” showing how a given star’s profile stabilizes with integration length. Tracing how progressively longer subaverages consistently approach, or diverge from, the form of the global average profile quantifies the number of pulses necessary for building a stable average profile. An average profile comprised of such a number of pulses constitutes a reliable signature and encompasses a pulsars behavior over a specific timescale. In practical terms, knowledge of stabilization rates facilitates optimal timing strategies with minimal timing residuals in order, for example, to determine binary orbits or attempt the detection of gravitational waves.

Following Helfand *et al.*, we then compute sets of av-

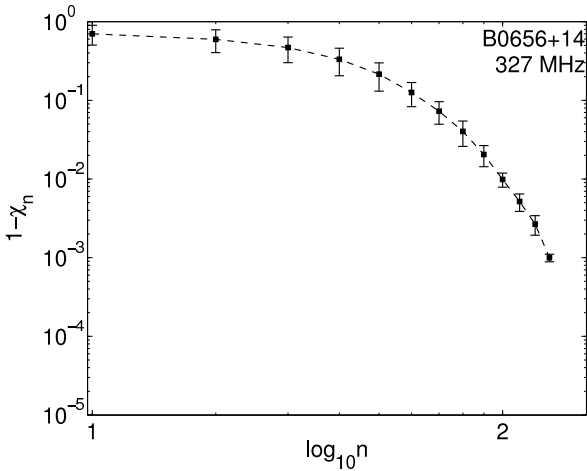
erage correlation coefficients χ_n for groups of both slow and millisecond pulsars by calculating the CCFs of each respective subaverage profile of n pulses with the global average profile. We then plot the quantities $1 - \chi_n$ versus n on a logarithmic scale in order to depict how a pulsars profile converges to a stable signature as the number of pulses used to construct the average increases. The minimum value of n for which χ_n is statistically significant is then interpreted as the most efficient integration length required for computing a stable average profile for a particular star.

Radio pulsars emit sequences of individual pulses—each one unique from the others and some nulled or “giant” as well as corrupted by radio-frequency interference—which can then be averaged synchronously to provide high signal-to-noise-ratio (hereafter S/N) profiles that exhibit remarkable stability over long periods of time. The four panels of Figure 1 exemplify how it is that the widely varied forms of single pulses, which almost never resemble a pulsars global average profile, nonetheless aggregate to it progressively. The example given here is for PSR J1740+1000, but this process obtains for the vast majority of stars. Notice that the block averages of pulses, as the averaged length increases, more closely resembles the global average profile. The observation in the figure represents a span of 4096 pulses, yet none of those exhibit profile forms close to that of the average profile, shown in the bottom panels of each set of subaverages.

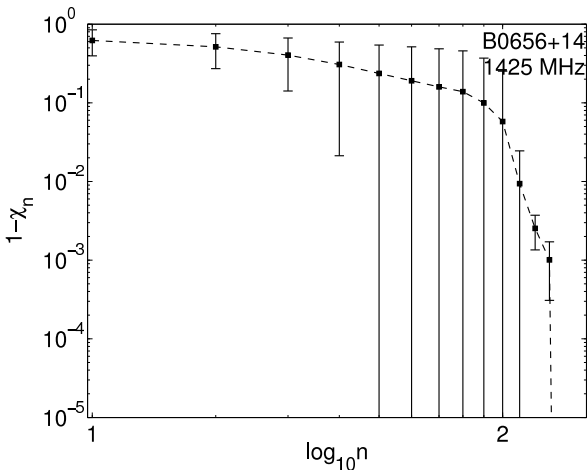
We can see in Fig. 1 that although the longer subaverage profiles bear more and more semblance to the global

* Mateus.Teixeira@uvm.edu; Joanna.Rankin@uvm.edu

Figure 1. Profile formation in pulsar J1740+1000: a) (left display) shows 128 single pulsars (main panel) together with their average subprofile (lower panel); b) (left central display) 32-pulse subprofiles together with their 1024-pulse subprofile; c) (right central display) 256-pulse subprofiles together with their 4096-pulse average profile; and d) (right display) two 1024-pulse subprofiles together with the the 4096-pulse average profile.



(a) B0656+14 P-band



(b) B0656+14 L-band

captionCorrelation analysis results for the respective P and L-band observations of pulsar B0656+14 in Table 1. Note the dramatic difference in profile dynamics.

average—*e.g.*, between the 32-pulse and the 1024-pulse subaverages—the number of pulses necessary to produce a subprofile/global average correlation that is statistically favorable for stability may not follow in a linear fashion. Indeed, it has been suggested that the stability curve may follow power laws, but this premise is tested strenuously only when the individual analyses for several stars show

convergence at both faster and slower rates. Our goal is to portray the cross-correlation coefficient as a means of quantifying the subaverage resemblance to the global average, such that one may find a number n of subaveraged pulses for which the profile may be considered stable.

Here, a primary motivation is that of including millisecond pulsars (hereafter MSPs) in our stability analysis for the first time. On the one hand, major efforts are in progress to construct pulsar timing arrays in order to search for gravitational waves (Foster & Backer 1990), and this requires further improvement of millisecond pulsar timing techniques. Specifically, in order to identify appropriate stars for membership in such arrays, criteria are needed to determine how well a particular star behaves as a cosmic clock, and a part of such assessment relates to profile stability. In short, we need measures both of the degree of stability and the rapidity of achieving it as both are relevant clock accuracy and its determination.

Paradoxically, we often know little about the individual pulse behavior of millisecond pulsars because the S/N is degraded simply by the necessity to sample them so rapidly. On the other hand, then, this effort offers some promise to explore whether faster stars also exhibit the nulling, moding and drifting behaviors often encountered in their slower counterparts. Such dynamic emission features have been largely overlooked thus far in the process of pulsar timing, especially in the timing of MSPs. Of course, the motivation for ignoring dynamical effects in timing efforts stems from the appearance that the average profiles of bright, normal pulsars remain stable enough to this end, though even here there is little systematic quantitative evidence to support this assumption.

Finally, the profile stabilization analysis is also pertinent to studying dynamic behaviors in “normal” pulsars, particularly because many such pulsars may also be analyzed on a single pulse basis, allowing for a consistency test between the correlation models and what one actually observes in the pulse sequences of such stars. Together, experience applying the correlation method to both normal pulsars and millisecond pulsars provides a more useful tool for assessing profile stability and a more powerful means of identifying dynamic behaviors in weak pulse sequences.

2 PROFILE CORRELATION ANALYSIS

The convergence rate of the CCF coefficient χ_n , computed from sub- and global average profiles of the total power (*i.e.*, Stokes parameter I), is the primary indica-

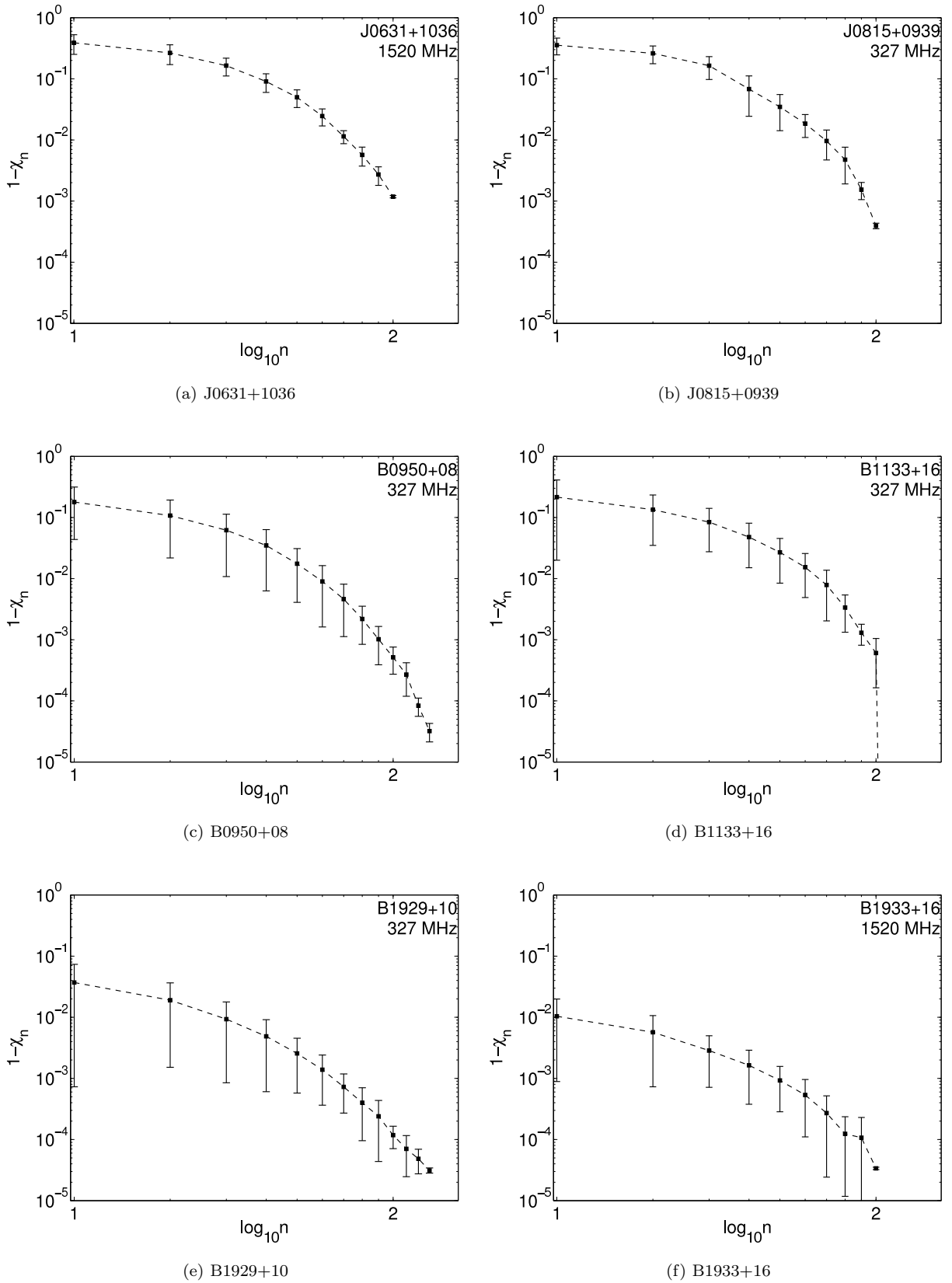


Figure 2. CS-MCMC analysis results for the six “normal” pulsars in Table 1. N.B. the x-axis labels here and in all the other plots are currently incorrect: “1” corresponds to 2^1 and “2” to 2^{10} or 1024. The single-pulse correlation 2^0 is not plotted.

tor of single pulse to average profile stabilization times. Given a global average profile of length G and subaverage profiles of length n , S_G and S_n respectively, the mean coefficient χ_n for cross correlations is given by

$$\chi_n = \frac{1}{N} \sum_{\alpha=1}^N \frac{\sum_i S_{nia} S_{Gi}}{\sqrt{\sum_i S_{nia}^2 \sum_i S_{Gi}^2}} \quad (1)$$

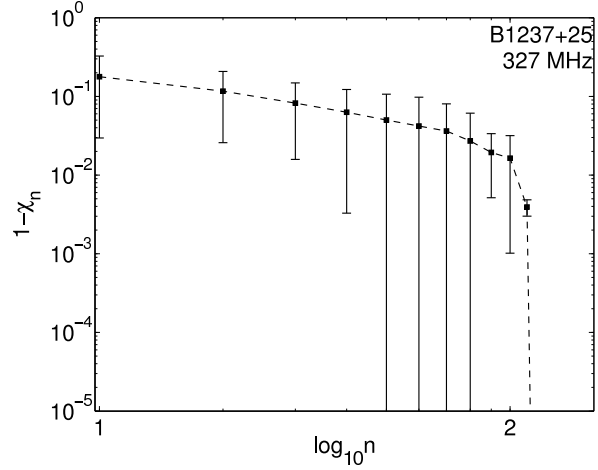
where $N = G/n$ modulo 2, and i stands for the bin index for the observation. As previously explained, the power law decay exhibited by the plot of $(1 - \chi_n)$ versus n tends to show distinct breaks in the slope for some pulsars, which often have coincided with the timescales of the aforementioned dynamic properties like drifting subpulses, moding, and nulling—but also with the overall complexity of the average profile (the intuitive reasoning suggesting that the more complex the profile, the slower or shallower the stabilization curve).

Both HMTIII and RR95 have shown that the stabilization rate of an individual pulsar corresponds not only with the presence of emission properties (*e.g.*, moding), but also to the time scales over which such properties manifest themselves. Even for stable, well studied pulsars, the stability curve has often seemed to follow power laws with two distinct slopes—a relatively shallow traverse at first and then a visibly steeper secondary slope at a characteristic integration length. Because these curves are of the form $(1 - \chi_n)$ versus n , the shallow slope occurs at n values for which the subaverages take longer to stabilize; consequently, the steeper slope at larger n values represents a break in the prior slope, at which point the pulsars profile stabilizes more rapidly, the quantity $(1 - \chi_n)$ approaching zero as the correlation coefficient tends to unity.

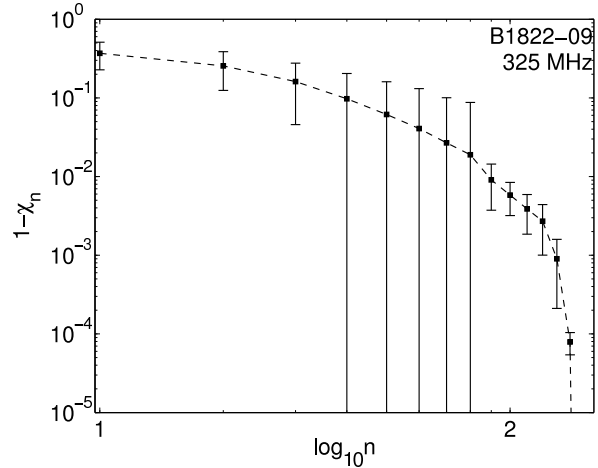
Not only that!—the timescale at which these slope breaks occur also coincides with timescales of dynamic effects like the drifting of subpulses and moding. A stabilization curve may in fact display more than one break in its slope if the particular star exhibits behaviors at different time scales. If such an analysis, carried out on a large enough population of slow and millisecond pulsars, reveals mode-changing and other emission properties in even a few of these stars, such knowledge would allow for better initial estimates and more accurate and precise construction of average profiles for timing applications.

3 OBSERVATIONS AND RESULTS

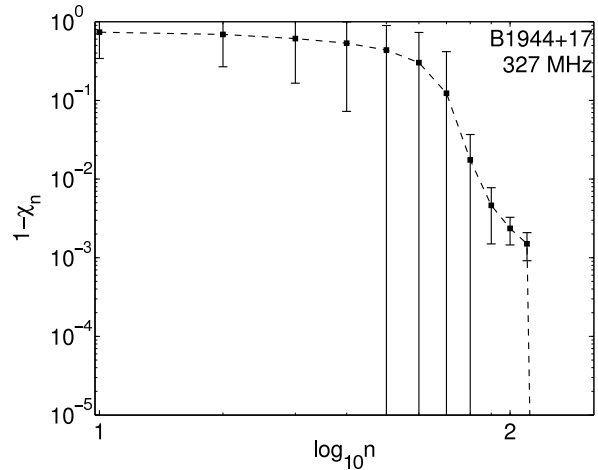
Altogether, eighteen observations of seventeen stars were used in the correlation analyses. All of the observations, with the exception of pulsars J0437–4715 and B1822–09, were made using the 305-m Arecibo Radio Observatory in Puerto Rico, at both 327 MHz and 1400 MHz (P- and L-bands, respectively). The observation of the millisecond pulsar J0437–4715 was conducted at 1375 MHz using the 64-m radio dish facility at the Parkes Observatory in New South Wales, Australia. The observations used



(c) B1237+25



(d) B1822-09



(e) B1944+17

Figure 3. Correlation analysis of 2012 RA 6, MNRAS 000, 1 of 7 changing pulsars in Table 1.

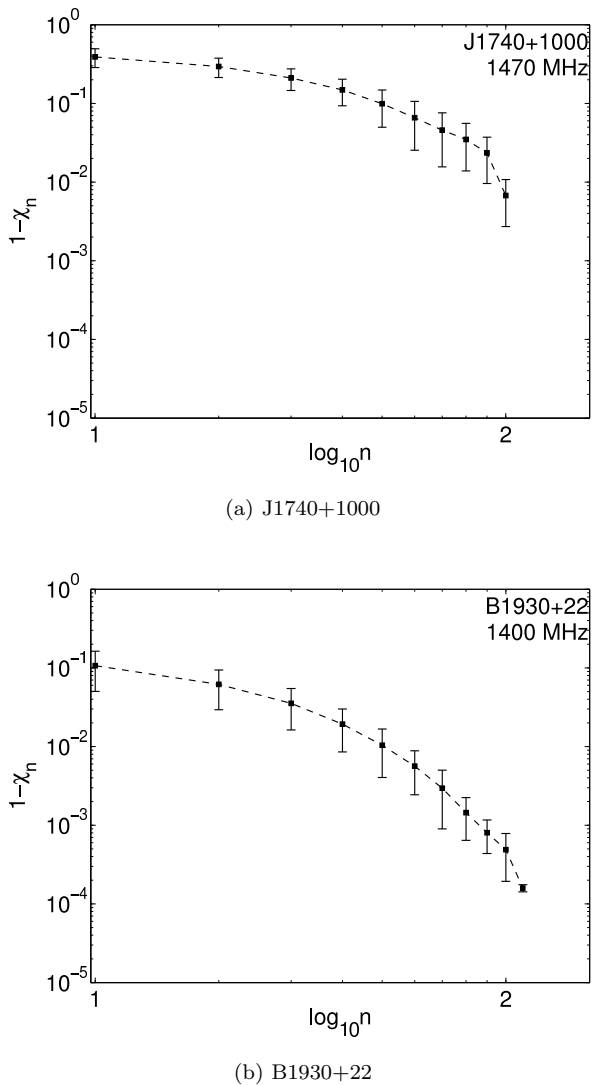


Figure 4. Correlation analysis results for the two fast pulsar observations in Table 1.

in the analysis of B1822–09 were made at 325 MHz by means of the Giant Metrewave Radio Telescope (GMRT) near Pune, India. The central frequency given on the correlation plots may not correspond exactly with the overall central frequency of each observation due to the fact that for some correlations specific bands were selected for mainly aesthetic and quality reasons. Table 1 lists each observation with their relevant details.

4 DISCUSSION

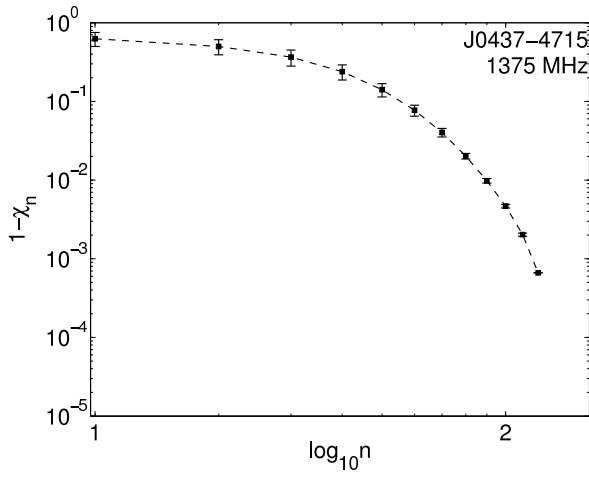
The plots in Figure 1 show the results of the algorithm outlined in Section 2 for the seventeen pulsars in Table 1, consisting of eighteen total observations—accounting for

both the P- and L-band information for PSR B0656+14. The error bars correspond to one standard deviation of the mean correlation coefficient χ , with errors extending beyond the plotted image due to the mathematical issue that in some correlations the sum of $(1 - \chi) - \sigma \leq 0$ implies that $\chi + \sigma \geq 1$. The awkwardness of defining these values on a logarithmic scale result in the blown up errors, which simply correspond to standard deviation values approaching the mathematical boundary. That the mean correlation coefficient χ deviates outside of unity is neither physically nor mathematically meaningful, and results from the statistical presumption that χ may be Gaussian-distributed, when in fact it likely occurs as a truncated Gaussian-distributed variable.

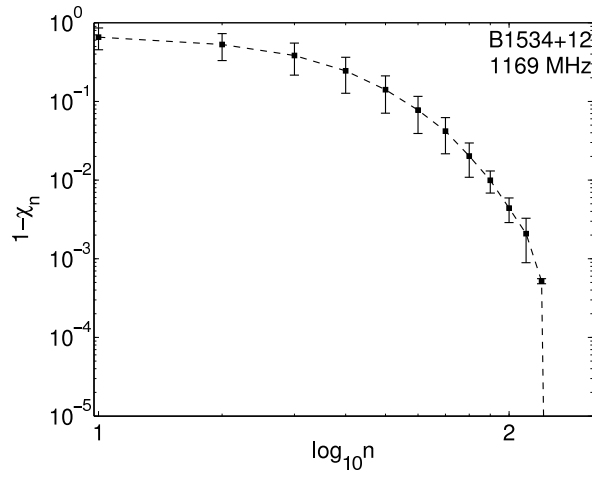
In the following sections we present our analysis results for groups of pulsars having either common pulse-sequence properties or similar stabilization characteristics.

Notable stars of the first kind, like the millisecond pulsars J0437–4715 and B1855+09, suggest highly stable profiles. J0437–4715 is in fact known to be one of the most stable and reliable timing pulsars yet discovered. Normal pulsars like the aforementioned J0815+0939 and J0631+1036 also appear relatively stable. On the case of the latter, a small flattening at the correlation of roughly 16-pulse subaverages hints at the drifting phenomenon in that order. Note also the similarity of the curves for PSRs B1930+22 and B1929+10, both of which have relatively high coefficient values for their first correlation, suggesting that individual pulses (or close: subaverages of two pulses) closely approximate the characteristic of a global profile. Both pulsars also stabilize rapidly, their curves behaving as power laws in n . PSR B1822–09s curve, as well as that for the L-band observation for B0656+14, suggest kinks that may suggest some instability, but a clear discussion is difficult due to the uncertainty in their respective errors, which blurs attempts at concrete classification. Most other pulsars in this group have small errors and are generally fast to stabilize on the order of subaverages containing more than 32 pulses.

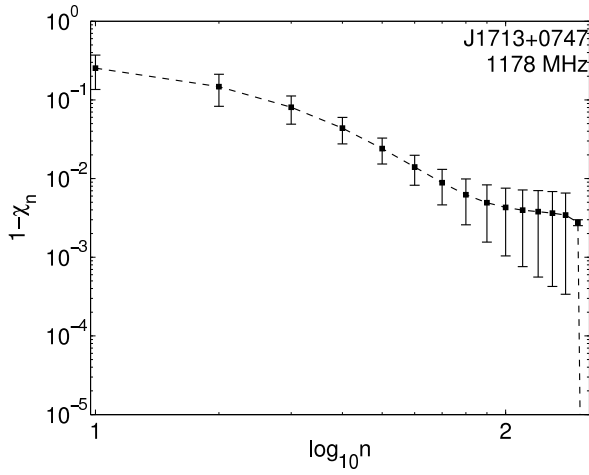
The less stable pulsar B1944+17 exhibits a dramatic slope break on the order of 128 pulses, which Kloumann notes occurs on the same order of magnitude as its mode changes [Kloumann Thesis, 2011]. Pulsars B1237+25, B1913+16, J1740+1000, and J1713+0747, regardless of whether they eventually stabilize (as is the case for J1740+1000), all show remarkably shallow stabilization curves, suggesting that even at large subaverage correlations, their profiles do not approach a global average very rapidly. PSR B1933+16 exhibits remarkable stability from the start, but suggests unstable features on the order of 256 pulses. In overall terms, this particular correlation would greatly benefit from lengthier observation times, such that this behavior could be traced to higher orders.



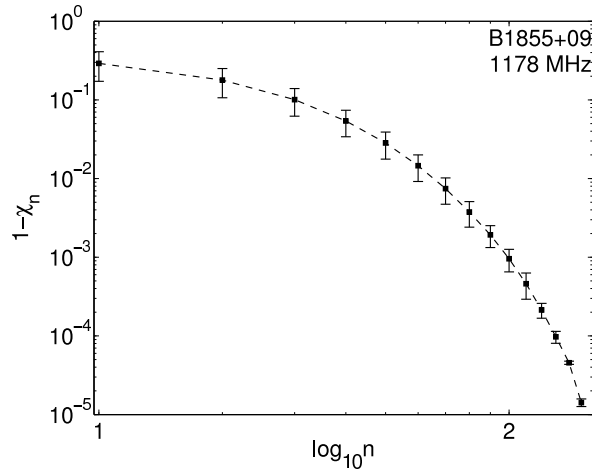
(a) J0437-4715



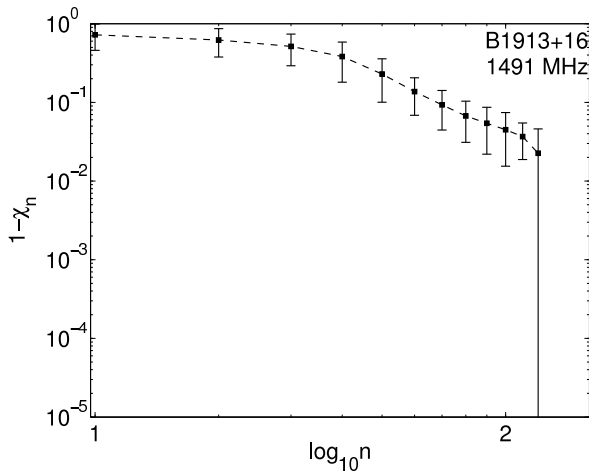
(b) B1534+12



(c) J1713+0747



(d) B1855+09



(e) B1913+16

Figure 5. Correlation analysis results for the five MSPs in Table 6 © 2012 RAS, MNRAS 000, 1–7

Table 1. The eighteen observations used in the correlation analyses.

| Pulsar | MJD | Frequency Band (MHz) | Pulsar Period (s) | S (mJy) | Number of Pulses |
|------------|-------|-------------------------|----------------------|---------|---------------------|
| J0437-4715 | 52004 | 1375 | 0.0058 | 142 | 9738 |
| J0631+1036 | 54540 | 1520 | 0.2878 | 0.8 | 3372 |
| B0656+14 | 52840 | 327 | 0.3849 | 6.5 | 24765 |
| B0656+14 | 53489 | 1525 | 0.3849 | 3.7 | 19107 |
| J0815+0939 | 54782 | 327 | 0.6451 | 3.7 | 3720 |
| B0950+08 | 53703 | 327 | 0.2530 | 400 | 23321 |
| B1133+16 | 53703 | 327 | 1.1878 | 257 | 2695 |
| B1237+25 | 53378 | 327 | 1.3823 | 110 | 5209 |
| B1534+12 | 55637 | 1169 | 0.0379 | 36 | 15835 |
| J1713+0747 | 55632 | 1178 | 0.0046 | 8 | 65646 |
| J1740+1000 | 54541 | 1470 | 0.1541 | 9.2 | 3894 |
| B1822-09 | 55014 | 325 | 0.7690 | 36 | 37399 |
| B1855+09 | 55637 | 1178 | 0.0054 | 5 | 111910 |
| B1913+16 | 55637 | 1491 | 0.0591 | 0.9 | 15233 |
| B1929+10 | 53186 | 327 | 0.2265 | 303 | 18835 |
| B1930+22 | 54540 | 1400 | 0.1445 | 1.2 | 4151 |
| B1933+16 | 54540 | 1520 | 0.3587 | 42 | 3352 |
| B1944+17 | 53966 | 327 | 0.4406 | 40 | 7038 |

ACKNOWLEDGMENTS

We are pleased to acknowledge Dipanjan Mitra and Geoff Wright for their critical readings of the manuscript. Portions of this work were carried out with support from US National Science Foundation Grants AST 99-87654 and 08-07691. The Arecibo Observatory is operated by SRI International under a cooperative agreement with the National Science Foundation, and in alliance with Ana G. Mndez-Universidad Metropolitana, and the Universities Space Research Association.. This work used the NASA ADS system.

REFERENCES

- Foster, R. S., & Backer, D. C. 1990, *Ap.J.*, 361, 300
Helfand, D. J., R. N. Manchester, and J. H. Taylor, 1975, *Ap.J.*, 198, 661-670 (HMTIII)
Kloumann, I. M., & Rankin, J. M. 2010, *MNRAS*, 408, 40
Latham, C. L., Mitra, D., & Rankin, J. M. 2012, *MNRAS*, in press
N. Rathnasree and J. M. Rankin, 1995, *Ap.J.*, 452, 814 (RR95)
Srostlik, Z., & Rankin, J. M., 2005, *MNRAS*, 362, 1121

This paper has been typeset from a $\text{\TeX}/\text{\LaTeX}$ file prepared by the author.